

Image Gradient Based Iris Recognition for Distantly Acquired Face Images Using Distance Classifiers

Arnab Mukherjee[1], Kazi Shah Nawaz Ripon[2(✉)], Lasker Ershad Ali[1(✉)], Md. Zahidul Islam[1], and G. M. Mamun-Al-Imran[1]

[1] Khulna University, Khulna, Bangladesh
ershad@math.ku.ac.bd
[2] Østfold University College, Halden, Norway
ksripon@hiof.no

Abstract. This paper presents an iris recognition framework to recognize irises from distantly acquired face images using image gradient-based feature extraction and K-Nearest Neighbor with various distance classifiers. The work herein applies the gradient local auto-correlation descriptor to extract discriminative features from the iris images and to reduce feature dimensionality by optimizing some parameters. Several distance metrics are applied in the iris classification stage to reduce computational complexity and build the classification models. The proposed framework effectively handles the noisy artefacts, rotation, occlusion, and illumination variation challenges. The experiments are carried out on a publicly accessible CASIA-V4 distance database to ascertain the effectiveness of distant iris recognition and to compare the efficacy of several existing distant classifiers. The experimental results justify that distance metrics influence the recognition outcomes of the classifier significantly, and the recognition performance of the Correlation distance metric is better than the other distance classifiers for iris gradient features.

Keywords: Iris recognition · Image gradient feature · Distance classifier · Local auto correlation feature descriptor · Distance metrics

1 Introduction

Iris recognition is one of the most automatic systems for recognizing or confirming an individual's identity swiftly, uniquely and reliably without the need for bearing or reminiscing anything, unlike conventional methods. Most security fields still follow the knowledge or token-based methods for individual identification. But those traditional methods, like username, password, personal identification numbers (PINs), credit cards, identification cards, and even passports, are susceptible to losing, conjecturing by a third party, forgetting, or damaging [23]. Recently, several studies have demonstrated that biometric technique is a promising solution for maximum security because biometric traits cannot be

© The Author(s), under exclusive license to Springer Nature Switzerland AG 2022
O. Gervasi et al. (Eds.): ICCSA 2022 Workshops, LNCS 13381, pp. 239–252, 2022.
https://doi.org/10.1007/978-3-031-10548-7_18

faked, borrowed, forgotten, stolen and guessed easily [4,19]. The main advantage of the biometric traits is that these are not forged practically [20]. Usually, biometrics are categorized into two groups: physiological and behavioural traits. Physiological traits include iris, facial thermo-grams, fingerprints, palm-prints, hand geometry, eyes, retina DNA, etc. In contrast, behavioural traits include gait, voice recording, human action, signature, handwriting, keystroke, rhythms, and the like [12].

The iris is regarded as the most reliable biometrics for human identification among various physiological traits. As the human iris is the only internal and external visible organ with its exclusive structure, it is highly protected from varied environmental conditions [8]. The construction of iris patterns is not related to genetic factors but somewhat arbitrary. Even a person's left and right irises are different due to a high degree of randomness and uniqueness of iris texture, and the irises of identical twins have no similarity [27]. Having rings, freckles, ridges, furrows, crypts, and zigzag patterns within the iris region are the causes of complexity in iris patterns. Also, the iris trait ensures a high degree of stability over a person's lifetime [7,8,12,20,23,27]. These desirable properties has motivated the researchers to consider the iris as the most secure and reliable biometric for high-security surveillance.

It is challenging to ensure the reliability of an automated system of identifying persons using the iris recognition system. This is because the eye images are captured in a controlled environment and a less controlled environment [20]. In a less controlled environment, the images are acquired at a longer distance from the subject, whereas the images are taken at short distances in a controlled environment. Under different imaging conditions, the distantly acquired iris images have motion blurs, occlusions owing to shadows, eyelashes and eyelids, lighting reflections, and other artefacts. These issues degrade the image quality significantly and cannot illustrate iris textures clearly in less controlled environments.

The iris recognition system still has various challenges like robust segmentation, appropriate feature extraction for distantly acquired noisy images, the computational complexity of classification, etc. Considering these challenges, this work focuses on developing an effective iris recognition framework by employing image gradient features, more specifically, local auto-correlation feature descriptor (GLAC) and distance classifiers. The novelty of the proposed framework is that the descriptor retrieves more informative features with lower dimensionality from the iris images of defocusing, motion blur, poor contrast and non-uniform illumination etc. Further, this work investigates the effectiveness of several existing distant classifiers within the K-Nearest Neighbor (K-NN)–based classifier. Experimental results suggest that the distance classifiers have the lowest noise implications and can enhance recognition accuracy and reduce the computational complexity of the iris recognition algorithm.

The remainder of this paper is organized as follows. Section 2 discusses iris recognition affiliated works briefly. Section 3 describes the Iris recognition framework, feature extraction strategy, and classification. Section 4 presents experimental measurement, results, and discussion. Finally, Sect. 5 concludes the paper.

2 Related Work

There is extensive literature on human identification, but the relevant papers on distant iris recognition are mentioned herein. John Daugman presented the first successful automated prototype of an iris recognition system using a 2D Gabor wavelet filter with hamming distance in 1994 [7]. Wildes et al. approached another prototype system employing Laplacian of Gaussian filter (LGF) with phase quantization at multiple scales and matched the binary features with normalized correlation [27]. Boles et al. considered the iris texture a zero-crossing of 1D dyadic wavelet filters for encoding iris patterns and recognized binary iris codes using Euclidean or Hamming distance [6]. Mukherjee et al. provided a comparative study on various distance measures by employing different types of mother wavelets on distance database in [18]. Noh et al. introduced a wavelet decomposition-based iris recognition system in [24]. Monro et al. encoded iris features using discrete cosine transform [17]. All these earlier attempts have focused on wavelet-based iris recognition systems with close distance images requiring equal high-quality iris textures and performing well under ideal imaging conditions. Moreover, the existing wavelet descriptors cannot retrieve multi-directional information. A contourlet transform to extract the intrinsic geometrical structures of iris patterns was proposed in [5] to address the drawback of wavelets. However, their recognition rate substantially decreases with increasing the number of subjects.

In 2017, Mahesh et al. provided a survey for the present scenario related to iris recognition works. Their survey included various practical techniques for iris image preprocessing, image segmentation, feature encoding, and iris classification, which were published from 2010 to 2015 [16]. Considering the need for remote human identification automatically, Fancourt et al. proposed the first distant image-based iris recognition at up to 10 m from the subject [11]. Hollingsworth et al. developed the best iris shift bit code using the fragile bit method, which worked effectively for distant iris images [13]. Dong et al. introduced a personalized weight map technique for iris matching [9]. Later, Tan and Kumar merged the fragile bit and personalized weight map techniques using the weighted sum method for classification [26]. Ali et al. established a composite feature descriptor including Log Gabor wavelet (LG), GLAC, Contourlet transformed (CT) and convolutional neural network (CNN) to enhance the recognition performance [2]. The feature-level fusion proposed in this work provides a promising solution for distance-based challenges. The same authors later provided an LG wavelet-based contourlet transform to overcome wavelet and contourlet transform limitations [3]. The feature descriptor retrieves two-dimensional singularities and spatial information more effectively in various directions than LG wavelet or contourlet transform. Still, it increases computational complexity in classification due to having high dimensionality for feature level fusion. In 2020, Tan and Domingo introduced an iris segmentation technique using a deep convolutional neural network [25]. The authors comprise encoder and decoder modules to enhance the iris segmentation performance for remotely captured iris or face images. However, the complete iris recognition framework is absent in their work.

Still, most of the existing iris recognition systems cannot provide any satisfactory outcome through their frameworks on varying levels of illumination, noisy and visible distant images. The work herein adopts the GLAC feature descriptor and distance-based classifier to overcome these shortcomings, which have robustness against low contrast and local illumination changes in the iris images.

3 Methodology

Figure 1 presents the block diagram for the proposed iris recognition framework. It includes the following key steps: eye image pre-processing, annular iris segmentation, iris feature extraction, classification, and iris recognition. The main contribution of the proposed framework is its computational simplicity due to the low order of local auto-correlation. Further, the investigation demonstrates that the Correlation distance metric may be employed instead of the usual Euclidean or Hamming distance for image patch matching, classification problems, object recognition, etc.

3.1 Image Pre-processing

During the acquisition process, the distant images suffer from non-uniform illumination, occlusions, and other noises. These artefacts present some difficulties in the iris segmentation and recognition stage. Thus, this work adopts a *Single Scale Retinex* (SSR) algorithm [3] to reduce the effect of uncontrolled light

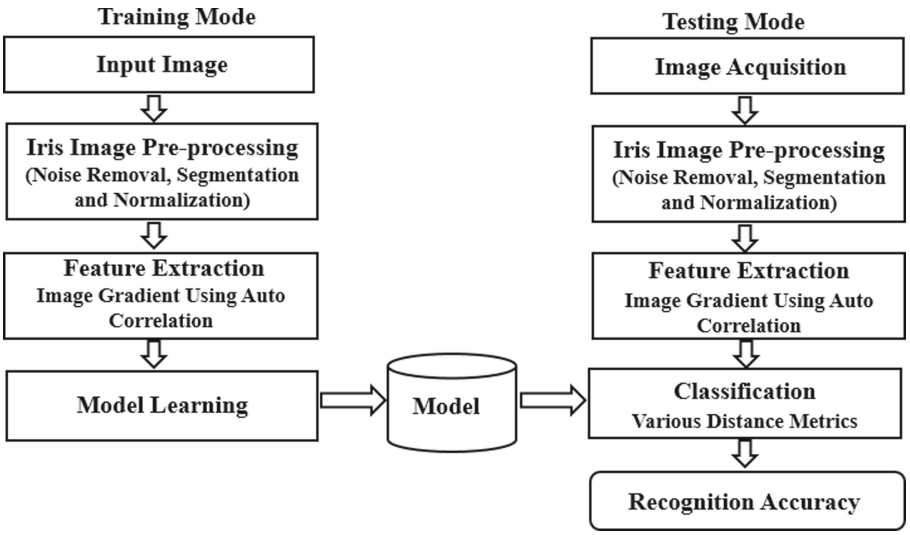

Fig. 1. The block diagram of the proposed iris recognition framework.

sources and improve the images' low contrast and sharpness. The general mathematical form of the algorithm is given by

$$R(u,v) = log\frac{Im(u,v)}{G_\tau{}^* Im(u,v)} \tag{1}$$

where, $Im(u,v)$ is a grey scale eye image, $G_\tau(u,v) = Cexp[-(u^2+u^2)/\tau^2]$ is a low pass Gaussian filter with standard deviation τ, and $*$ is the convolutional operator.

3.2 Iris Segmentation

A robust and efficient segmentation algorithm can significantly enhance the distant iris recognition performance. The work herein utilizes a *Random Walker* (RW) algorithm to obtain coarse iris segmentation through a set of post-processing operations as detailed in [3]. It provides the iris texture and corresponding binary iris mask. The proposed framework also applies a circular model to localize approximately the boundaries of pupillary and limbic as the binary masks cannot inform details about the boundaries. The segmentation phase is finished after eliminating the occlusion noises, for example, eyelids, eyelashes and shadow.

3.3 Iris Normalization

As mentioned earlier, iris sizes vary from person to person, even both person's irises. These occur by the dilation and contraction of the pupil with variations in illumination. Such elastic distortions of iris texture influence the recognition results. So, it is expedient to compensate for those distortions to extract more accurate features. To account for the issues, the proposed framework applies the *Daugman's Rubber Sheet Model* [7] to normalize the segmented iris by constructing a remapping from Cartesian to dimensionless polar coordinates. The complete iris pre-processing steps are presented sequentially in Fig. 2.

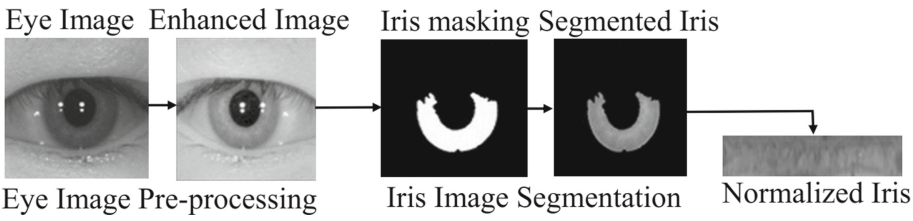

Fig. 2. The schema of eye image pre-processing to iris normalization.

3.4 Gradient Feature Extraction

The gradient local auto-correlation (GLAC) feature descriptor is a relatively newer feature descriptor for iris recognition. This shift-invariant descriptor was proposed by Kobayashi and Otsu [14] as a root extension scale Invariant and feature transform (SIFT) or histogram of oriented gradients (HOG). If $Im(u, v)$ be a 2-dimensional iris image region with a position vector $p = (u, v)^t$ on Im, the image gradients $(\frac{\partial G}{\partial u}, \frac{\partial G}{\partial v})$ are computed with any gradient filters, like Sobel, Prewitt, Roberts filter, and one-dimensional derivatives $[-1, 0, 1]$ and $[-1, 0, 1]^T$. At the point $Im(u, v)$, the gradient norm and oriented vector can be expressed as $m = |\Delta G(u, v)| = \sqrt{(\frac{\partial G}{\partial u})^2 + (\frac{\partial G}{\partial v})^2}$ and $\theta = \tan^{-1}(\frac{\partial G}{\partial v} / \frac{\partial G}{\partial u})$, respectively [16]. The oriented angle θ is coded into D-orientational bins by casting weighted votes to the closest bins. The orientational bins construct a D-dimensional gradient oriented G-O vector with g. In other words, the vector is a sparse vector of $g \in R^D$, and the G-O vectors are sparsely defined in terms of their norms and oriented angles. With the gradient norm m and G-O vector g, the Nth order gradient auto-correlation function around the local neighbors is given by

$$R(d_0, d_1, d_2.....d_N, f_0, f_1, f_2, ..., f_N) = \int_{Im} \omega[m(p), m(p + f_1), ..., m(p + f_N)] \\ g_{d_0}(p) g_{d_1}(p + f_1).....g_{d_N}(p + f_N) dp \tag{2}$$

where, the displacement vectors $f_1, f_2, f_3.....f_N$ are known as shifting vectors with respect to the location vector from the reference point $p(u, v)$ of each pixel in Im, and $m(p)$ is the norm of p. The scalar function $\omega(.)$ is used as the weights of auto-correlation, which is derived from norm m functions and g_d is the dth element of g.

There have two types of gradient correlations in Eq. 2: (i) orientational correlations obtained from the products of the element values g_{d_i} and (ii) spatial correlations attained from displacement vectors f_i. Equation 2 can be taken in various forms by changing the values of N, f_i and ω. According to the suggestion in [2], the experiments in this work considers $N \in \{0, 1\}$, $f_{1x,y} \in \{\pm \Delta p, 0\}$ and $\omega(.) = min$. The formulation of 0th and 1st order GLAC features are as follows:

$$F_0 : R_{N=0}(d_0) = \sum_{p \in Im} m(p) g_{d_0}(p) \tag{3}$$

$$F_1 : R_{N=1}(d_0, d_1, f_1) = \sum_{p \in Im} min[m(p), m(p + f_1)] g_{d_0}(p) g_{d_1}(p + f_1) \tag{4}$$

The spatial auto-correlations are computed by applying the mask patterns of $(p, p+f_1)$. There exists only one mask pattern in Eq. 3, and four individual mask patterns in Eq. 4 for computing the auto-correlations by avoiding duplicates that arise from shifts. The mask patterns to compute the element values of G-O vector pairs are mentioned in Algorithm 1.

Finally, all the elements for the 1st order are multiplied and summed over the image region. Although the GLAC feature dimension vector (concerning

F_0 and F_1 in $D + 4D^2$) is large, its feature vector computation is not so high because of the sparseness G-O vector g. Since the sparseness of$g$ is independent of orientational bins D, the computational cost is also invariant to the number of D.

Algorithm 1: Basic Algorithm of GLAC Computation

Pre-processing: The gradient norm m and G-O vector g are computed from the image gradients;
0th **Order GLAC:** In Eq. (3), summation is taken to two non-zero elements of the G-O vector g with weight $m(p)$ only at each pixel g;
1st **Order GLAC:** In Eq. (4), summation are taken by multiplying the non-zero elements of $g(p)$ and $g(p + f_1)$ with weight of $min[m(p), m(p + f_1)]$ for each mask pattern at p. Only four times multiplication requires for this operation;

3.5 Classification

K-Nearest Neighbor (K-NN) is a distance-based supervised classifier that assigns a label to classify the test iris image based on the majority vote of its K-nearest neighbours, which are closest to the test image. If $u = (u_1, u_2, u_3, ..., u_n)$ and $v = (v_1, v_2, v_3, ..., v_n) \in R^n$ be two feature vectors in a multi-dimensional feature space, then the distance metrics tested in this work – Euclidean (Eucl), standardized Euclidean (Steu), Minkowski (Min), city block (City), Chebychev (Cheb), cosine (Cos), correlation (Cor), Hamming (Ham) and Spearman (Spr), can be defined as follows:

$$D_{Eucl}(u, v) = \sqrt{\sum_{i=1}^{n}(u_i - v_i)^2} \tag{5}$$

$$D_{Steu}(u, v) = \sqrt{\sum_{i=1}^{n}(u_i - v_i)^2/s^2} \tag{6}$$

where, s_i is the standard deviation of the u_i and v_i over the feature sets.

$$D_{Min}(u, v) = \sqrt[r]{\sum_{i=1}^{n}|u_i - v_i|^r} \tag{7}$$

$$D_{City}(u, v) = \sum_{i=1}^{n}|u_i - v_i| \tag{8}$$

$$D_{Cheb}(u, v) = \max_i \ |u_i - v_i|, \tag{9}$$

$$D_{Spr}(u, v) = 1 - \frac{\sum_{i=1}^{n}(u_i' - \overline{u_i}')(v_i' - \overline{v_i}')}{\sqrt{\sum_{i=1}^{n}(u_i' - \overline{u_i}')^2 \sum_{i=1}^{n}(v_i' - \overline{v_i}')^2}} \tag{10}$$

where, ${u_i}'$ is the tied rank of u_i and $\overline{u}' = \frac{1}{n}\sum_{i=1}^{n} {u_i}'$; and ${v_i}'$ is the tied rank of v_i and $\overline{v}' = \frac{1}{n}\sum_{i=1}^{n} {v_i}'$

$$D_{Cos}(u, v) = 1 - \frac{\sum_{i=1}^{n} u_i v_i}{\sqrt{\sum_{i=1}^{n} {u_i}^2 \sum_{i=1}^{n} {v_i}^2}} \tag{11}$$

$$D_{Cor}(u, v) = 1 - \frac{\sum_{i=1}^{n} (u_i - \overline{u_i})(v_i - \overline{v_i})}{\sqrt{\sum_{i=1}^{n} (u_i - \overline{u_i})^2 \sum_{i=1}^{n} (v_i - \overline{v_i})^2}} \tag{12}$$

$$D_{Ham}(u, v) = \frac{1}{n} \sum_{i=1}^{n} (u_i \neq v_i) \tag{13}$$

4 Experiments and Results

The experiments are carried out on the CASIA-V4 distance database – the largest open-source database for distantly acquired facial images [1]. The Chinese Academy of Science's Institute of Automation (CASIA) has released this database for secure biometrics recognition. The complete database is made up of 2,567 facial images with 142 subjects, including regular and more complicated images in most subjects. A Near-Infrared camera acquires the facial images in less controlled environments at 3 meters distance from the subject.

For the experiments in this work, firstly, the eye images are isolated from the whole facial images and are obtained 5,134 images, including left and right eye images. It was not possible to isolate all the eye images correctly from the facial images due to containing eyes with glasses, reflections, hair, or other noise factors. This work does not consider the regular images of the first 14 subjects to enhance the reliability of the proposed system. From each of the remaining 128 subjects, a total of 3,041 randomly chosen images are selected as training images. Similarly, 712 images are selected as test images. The experiments are implemented using MATLAB R2018a (Intel core i5) and python 3.7.

The proposed framework applies the GLAC descriptor to extract informative iris features by customizing some parameters. All the features are normalized, adopting the min-max normalization technique in the data pre-processing stage [3]. All the training images are employed to train the classifier and test images for classification. As mentioned earlier, distance metrics are used to build the K-NN classification models. The average precision, recall, F_1-measure values from the confusion matrix are computed for each distance metric and other gradient feature descriptors to evaluate and compare the classification performance, as shown in Table 1.

Table 1. Performance of distance metrics on GLAC features.

Distance metrics	Avg. precision	Avg. recall	F1-measure	Accuracy (%)
Euclidean distance	0.9124	0.8956	0.8918	89.59
Minkowski distance	0.9124	0.8956	0.8917	89.59
City block distance	0.9151	0.8992	0.8961	90.02
Chebychev distance	0.6595	0.6380	0.6210	63.99
Spearman distance	0.9169	0.9153	0.9059	91.56
Cosine distance	0.9015	0.9019	0.8908	90.02
Correlation distance	**0.9139**	**0.9175**	**0.9073**	**91.84**
Standardized Euclidean distance	0.8625	0.8373	0.8306	84.24
Hamming distance	0.9105	0.8942	0.8868	89.45

4.1 Performance Study

The recognition performance is analyzed sequentially by changing parameter values. The key parameters are: (*i*) Roberts cross operator; (*ii*) 17 Orientation bins over [0°, 180°) (unsigned gradients); (*iii*) Spatial interval $\Delta p = 5$ with 1st order auto correlation; (*iv*) 4×5 Spatial bins and L_2-Hys block normalization.

Initially, all the gradient orientated vectors are computed across the iris image by convolving with gradient operators such as Roberts, one-dimensional derivatives [−1, 0, 1], Prewitt, and Sobel operators. Figure 3 presents the comparative results. The performance of Roberts's operator is more compact and effective than other operators, whereas the Prewitt operator is least effective, as illustrated in Fig. 3. Finally, the gradient orientations are quantized into 17 bins and follow the min-weighted function to suppress the noisy effect on surrounding auto-correlations. The orientation bins are equally spread over $[0°, 180°)$ (unsigned gradients) or $[0°, 360°)$ (signed gradients). The unsigned gradient always performs better than the signed gradient for auto-correlations of orientations, as depicted in Fig. 4.

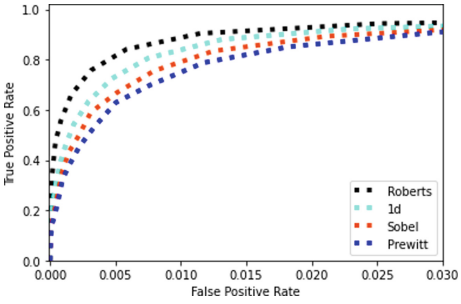

Fig. 3. ROC curves for gradient operators

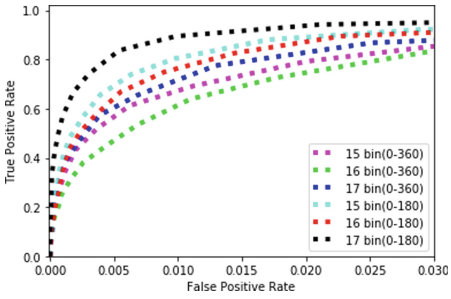

Fig. 4. ROC curves for different orientation bins

From Fig. 3 and Fig. 4, it can be observed that the auto-correlations of orientations depend on spatial interval Δp, which is highly correlated with the scale of images that would be recognized. The order of gradient auto-correlation also influences the GLAC configuration and increases feature dimensionality with higher running time. Although small spatial intervals work better with local auto-correlations, the spatial interval performs well in the case of 1st order component with the Roberts filter, as shown in Fig. 5.

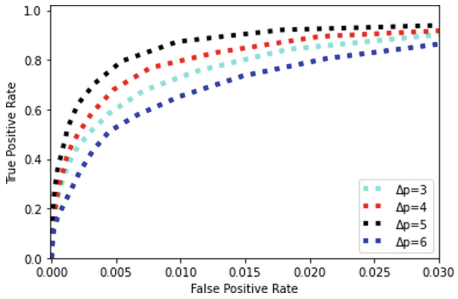

Fig. 5. ROC curves for special intervals

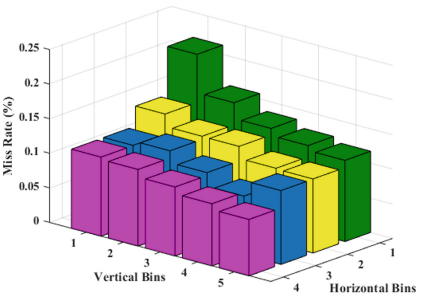

Fig. 6. Block diagram for special bins

The coarser spatial binning is adopted for the high dimensionality of gradient features, equally spaced over the normalized iris image. Among the spatial bins, the performance of spatial bins is the most effective as the spatial binning increases discriminative power by reducing shift-invariance. The spatial bins 3×4 also result in a good performance but not as good as spatial bins 4×5, as illustrated in Fig. 6.

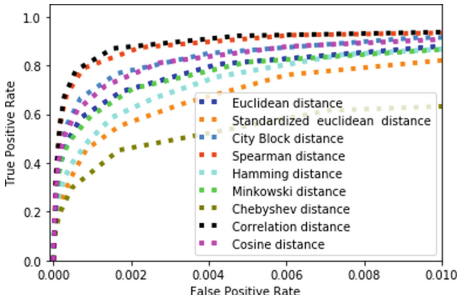

Fig. 7. Various distance metrics based ROC curves

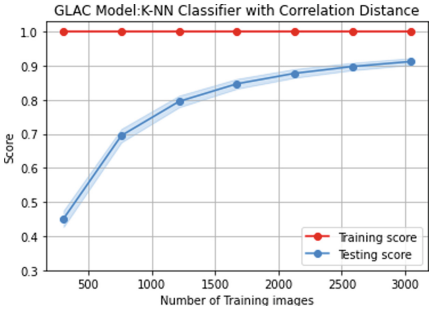

Fig. 8. Learning curves (Color figure online)

Figure 7 shows the performance comparisons for the distance matrices. As shown in this figure, the Correlation distance is the most compact and effective

metric for the K-NN classifier among the distance metrics for image gradient features. The values mentioned in Table 1 also confirms this. As shown in the figure and Table, the Correlation distance metric slightly improves performance by around 2.25%, compared to the most widely used Euclidean distance metric. And, the performance of Chebychev distance is always the least effective. Figure 7 shows that Euclidean and Minkowski distance metrics perform equally well. In contrast, the accuracies of city block and cosine distance metrics are almost the same, but the performance of city block distance is significantly better than cosine distance. The Chebychev and standardized Euclidean distance metrics perform at the cost of a much longer run time.

In addition, the parameter tuning during the experiments implies that the image gradient features are not uniformly distributed and have more non-linearity between training and test features. It indicates that most subjects have noisy, complicated eye images with light reflection. The proposed framework could not recognize iris features accurately in those subjects. In addition, the parameter tuning during the experiments implies that the image gradient features are not uniformly distributed and have more non-linearity between training and test features.

Table 2. Accuracies achieved by different gradient features based iris recognition approaches.

Feature descriptor	Avg. precision	Avg. recall	F1-measure	Accuracy (%)
EOH	0.7784	0.7786	0.7595	77.95
HOG	0.9012	0.8899	0.8761	89.03
GLBP	0.9171	0.8949	0.8901	89.87
STACOG	0.7399	0.7113	0.6953	71.17
GLAC	**0.9139**	**0.9175**	**0.9073**	**91.84**

Table 2 presents the performance comparisons of the proposed feature descriptor (GLAC) against the state-of-the-art gradient and standard histogram-based feature descriptors, namely space-time auto-correlation of gradients (STACOG), edge orientation histograms (EOH), rotational invariant gradient local binary pattern (GLBP) and histogram of oriented gradients (HOG). As shown in the Table, the proposed gradient feature descriptor achieves the highest recognition rate of 91.84%, reducing longer running time.

Figure 8 plots the learning curves of the K-NN model with Correlation distance that employs the gradient auto-correlation features. The boldface line for the test scores refers to the mean scores, and the shaded region surrounding the line denotes the range of its standard deviation. The red and cyan colour curves indicate the training and testing scores. It is visible from Fig. 8 that the learning curve converses at a good score, which suggests that the GLAC model is not under-fitting. It is also noticeable that the training scores are always high along with the iterations, and the testing scores will be enhanced by increasing the training images.

Table 3. Performance evaluation with competitive methods.

Research methods	Accuracy (%)
Symlet Wavelet and Spearman distance [18]	78.38
Local Binary Pattern and Euclidean distance [22]	84.88
Gray Level Co-Occurrence Matrix and Euclidean distance [10]	85.00
Contourlet Transform and Hamming distance [5]	86.40
Laplacian of Gaussian filters and Normalized correlation [27]	86.49
Convolutional Neural Network and Euclidean distance [2]	86.94
Principal Component Analysis and City block distance [21]	90.00
Monogenic Log Gabor filter and normalized Hamming distance [15]	90.43
Gradient Local Auto-correlation and Correlation distance (Proposed)	**91.84**

Table 3 compares the overall recognition accuracy of the proposed GLAC descriptor against the existing competing approaches. It should be mentioned that it is not feasible to directly compare the achieved results of the proposed framework with those of the existing models. This is because the proposed framework has adopted different strategies in iris segmentation, feature extraction and classification on various types of databases with different distributions. For example, the accuracies obtained in [5] are 86.40% for 100 subjects, 92.50% for 60 subjects and 96.50% for 20 subjects on CASIA-V1 iris database. Only the approach proposed in [2] and [3] experimented on a distantly acquired complicated database with a large number of images and subjects similar to this work. In [2], the authors reported several achieved values for efficiency using different feature fusion techniques. Among those values, there is a reported efficiency of 98.17%. However, this efficiency is not directly comparable to the efficiency achieved in this work. This is because the reported efficiency of 98.17% in [2] is based not only on the iris, like our approach, but also on the contextual eye, including the sclera, eyelid, pupil, eyelash, etc. The value (86.94%) mentioned in Table 3 for [2] is the efficiency acquired by using the actual iris and Euclidean distance-based method (K-NN), which is comparable to this work.

Several distance-based human identification techniques using only eye images are available in the existing literature. However, most of them are not completely based on iris texture. For example, the approach presented in [20] is a deep feature-based eye recognition for human identification. In addition, the experiments in this work include multiple noisy sources, occlusions and more complicated images with specular or light reflection in each subject. However, the comparative evaluations against earlier approaches identify that the proposed framework is highly effective and robust for remote human identification in the perspective of image conditions, as compared with other gradient and distance-based approaches.

5 Conclusion

This paper proposes a robust iris recognition framework for distant iris images in less controlled environments. The experimental results suggest that the proposed framework works effectively on local image gradients with spatial and oriented auto-correlations. The comparisons with the existing approaches also indicate that it performs better under varying imaging conditions than other gradient-oriented approaches. This work also investigates the performances of several existing distant classifiers. The results justify that the recognition rate of the K-NN classifier is improved slightly by choosing distance metrics depending on feature properties and image conditions. Further, this work studies the influence of various parameter settings and finds the optimal parameters for reliable performance. In future, it is essential to overrate the iris pre-processing stage for accurate iris segmentation by mitigating the influence of noisy artefacts such as non-uniform illumination, eyelash, and eyelid. A further natural extension is to employ feature fusion, selection and robust classifiers to overcome the inter-class ambiguities and enhance the overall recognition performance for the iris images acquired using visible or near-infrared illumination.

References

1. Biometrics ideal test CASIA iris image database (2011). http://biometrics.idealtest.org/. Accessed 28 Apr 2022
2. Ali, L.E., Luo, J., Ma, J.: Iris recognition from distant images based on multiple feature descriptors and classifiers. In: 2016 IEEE 13th International Conference on Signal Processing (ICSP), pp. 1357–1362. IEEE (2016)
3. Ali, L.E., Luo, J., Ma, J.: Effective iris recognition for distant images using log-Gabor wavelet based contourlet transform features. In: Huang, D.-S., Bevilacqua, V., Premaratne, P., Gupta, P. (eds.) ICIC 2017. LNCS, vol. 10361, pp. 293–303. Springer, Cham (2017). https://doi.org/10.1007/978-3-319-63309-1_27
4. Arora, S., Bhatia, M.: Challenges and opportunities in biometric security: a survey. Inf. Secur. J. Glob. Perspect. **31**(1), 28–48 (2022)
5. Azizi, A., Pourreza, H.R.: A new method for iris recognition based on contourlet transform and non linear approximation coefficients. In: Huang, D.-S., Jo, K.-H., Lee, H.-H., Kang, H.-J., Bevilacqua, V. (eds.) ICIC 2009. LNCS, vol. 5754, pp. 307–316. Springer, Heidelberg (2009). https://doi.org/10.1007/978-3-642-04070-2_35
6. Boles, W.W., Boashash, B.: A human identification technique using images of the iris and wavelet transform. IEEE Trans. Sig. Process. **46**(4), 1185–1188 (1998)
7. Daugman, J.: How iris recognition works. In: The Essential Guide to Image Processing, pp. 715–739. Elsevier (2009)
8. Daugman, J.: Information theory and the iriscode. IEEE Trans. Inf. Forensics Secur. **11**(2), 400–409 (2015)
9. Dong, W., Sun, Z., Tan, T.: Iris matching based on personalized weight map. IEEE Trans. Pattern Anal. Mach. Intell. **33**(9), 1744–1757 (2010)
10. Emrullah, A.: Extraction of texture features from local iris areas by GLCM and iris recognition system based on KNN. Eur. J. Tech. (EJT) **6**(1), 44–52 (2016)

11. Fancourt, C., et al.: Iris recognition at a distance. In: Kanade, T., Jain, A., Ratha, N.K. (eds.) AVBPA 2005. LNCS, vol. 3546, pp. 1–13. Springer, Heidelberg (2005). https://doi.org/10.1007/11527923_1
12. Hamouchene, I., Aouat, S.: Efficient approach for iris recognition. SIViP **10**(7), 1361–1367 (2016). https://doi.org/10.1007/s11760-016-0900-y
13. Hollingsworth, K.P., Bowyer, K.W., Flynn, P.J.: The best bits in an iris code. IEEE Trans. Pattern Anal. Mach. Intell. **31**(6), 964–973 (2008)
14. Kobayashi, T., Otsu, N.: Image feature extraction using gradient local auto-correlations. In: Forsyth, D., Torr, P., Zisserman, A. (eds.) ECCV 2008. LNCS, vol. 5302, pp. 346–358. Springer, Heidelberg (2008). https://doi.org/10.1007/978-3-540-88682-2_27
15. Kumar, A., Chan, T.S., Tan, C.W.: Human identification from at-a-distance face images using sparse representation of local iris features. In: 2012 5th IAPR International Conference on Biometrics (ICB), pp. 303–309. IEEE (2012)
16. Mahesh, K.K., Kishore, P., Kailash, J.K.: Survey on iris image analysis. Indian J. Sci. Technol. **10**(9), 1–15 (2017)
17. Monro, D.M., Rakshit, S., Zhang, D.: DCT-based iris recognition. IEEE Trans. Pattern Anal. Mach. Intell. **29**(4), 586–595 (2007)
18. Mukherjee, A., Islam, M.Z., Mamun-Al-Imran, G., Ali, L.E.: Iris recognition using wavelet features and various distance based classification. In: 2021 International Conference on Electronics, Communications and Information Technology (ICECIT), pp. 1–4. IEEE (2021)
19. Ngo, D.C.L., Teoh, A.B.J., Hu, J.: Biometric Security. Cambridge Scholars Publishing, Cambridge (2015)
20. Ripon, K.S.N., Ali, L.E., Siddique, N., Ma, J.: Convolutional neural network based eye recognition from distantly acquired face images for human identification. In: 2019 International Joint Conference on Neural Networks (IJCNN), pp. 1–8. IEEE (2019)
21. Sari, Y., Alkaff, M., Pramunendar, R.A.: Iris recognition based on distance similarity and PCA. In: AIP Conference Proceedings, vol. 1977, p. 020044. AIP Publishing LLC (2018)
22. Sarode, N.S., Patil, A., Nssdam, P.: Iris recognition using LBP with classifiers-KNN and NB. Int. J. Sci. Res. **4**(1), 1904–1908 (2015)
23. Savoj, M., Monadjemi, S.A.: Iris localization using circle and fuzzy circle detection method. World Acad. Sci. Eng. Technol. (61), 2 (2012)
24. Seung-In, N., Bae, K., Park, Y., Kim, J.: A novel method to extract features for iris recognition system. In: Kittler, J., Nixon, M.S. (eds.) AVBPA 2003. LNCS, vol. 2688, pp. 862–868. Springer, Heidelberg (2003). https://doi.org/10.1007/3-540-44887-X_100
25. Tan, C.W., Domingo, S.T.: Accurate iris segmentation for at-a-distance acquired iris/face images under less constrained environment. In: Proceedings of the 2020 International Conference on Pattern Recognition and Intelligent Systems, pp. 1–5 (2020)
26. Tan, C.W., Kumar, A.: Accurate iris recognition at a distance using stabilized iris encoding and Zernike moments phase features. IEEE Trans. Image Process. **23**(9), 3962–3974 (2014)
27. Wildes, R.P.: Iris recognition: an emerging biometric technology. Proc. IEEE **85**(9), 1348–1363 (1997)